Kinetics of the Heterogeneous Decomposition of Nickel Tetracarbonyl

HERBERT E. CARLTON and JOSEPH H. OXLEY

Battelle Memorial Institute, Columbus, Ohio

The decomposition of nickel tetracarbonyl at pressures between 20 and 200 torrs was studied at temperatures from 100° to 225°C. In the cross-flow system, the rate in the absence of appreciable dilution was primarily limited by kinetic resistances at temperatures up to about 175°C. over an effective Reynolds number range of 5 to 100. Gas phase diffusional resistances were controlling at higher temperatures. Corrections for natural convection were employed in both the kinetic and diffusional regions of control.

A series of chemical reactions in a differential reaction system is being studied to provide boundary conditions for multicomponent mass transfer correlations in convective flow systems. By following the methods used previously to correlate rates in the kinetically controlled region for the deposition of iron from its pentacarbonyl (*1*), a similar study has been made of the deposition of nickel from its tetracarbonyl. The use of nickel carbonyl in this experimental work has most of the advantages of that of iron carbonyl, except that nickel carbonyl is extremely toxic and extensive safety precautions are necessary when it is employed. The maximum allowable concentration of nickel carbonyl which can be inhaled for long periods of time has been tentatively set at 1 p.p.b. (*2*).

Nickel tetracarbonyl decomposes according to the overall equation

$$Ni(CO)_4 \rightarrow Ni + 4CO \qquad (1)$$

This reaction is of considerable interest commercially and, shortly after it was discovered by Mond in 1889 (*3*), it was employed as the basis for the large nickel refinery at Clydach, England (*4*).

The previously reported experimental work on nickel carbonyl is extensive. The pioneering work of Mittasch (*5*) is still one of the more valuable references. He reported that the reaction was of first order at low temperatures. Bawn (*6*), Garratt and Thompson (*7*), and Tonosaki (*8*) studied the decomposition reaction in a uniformly heated sealed bulb and measured pressure change with time. Some of these investigators recognized, and Chan and McIntosh (*9*) demonstrated, that the rate measured in a static system was not only a function of surface area, but also of reactor volume and therefore the rate limiting steps in the decomposition could involve homogeneous as well as heterogeneous reaction. Tewes, Zava, and Hoover (*10*) and Boettger and Fetting (*11*) measured decomposition rates in flow systems. A first-order reaction was assumed by the latter investigators. Verblovskii and Rotinian (*12*) obtained a linear relationship between growth rates of nickel deposits and nickel carbonyl concentration (and hence partial pressure), but for practical reasons they operated at conditions where high conversions were obtained and apparent first-order behavior would be expected. Owen (*13*) described the coatings deposited under a wide variety of conditions, and Callear (*14*) investigated the photochemical decomposition of nickel carbonyl. The patent literature is quite extensive and the interested reader should refer to the survey paper by Mond (*15*), and the books by Belozerskiy (*16*) and by Powell, Campbell, and Gonser (*17*) for comprehensive bibliographies. However, in no case has a sufficiently detailed analysis of the process been made which will permit confident extrapolation of heterogeneous kinetic data into the regions dominated by gas phase mass transfer considerations. This study was therefore carried out to supply this information.

THERMODYNAMIC ANALYSIS

The equilibrium conversion of nickel carbonyl to nickel and carbon monoxide is shown in Figure 1. Equilibrium yields were calculated from $\Delta F_{298} = 5.5$ kcal. as presented by Spice, Staveley, and Harrow (*18*), and $\partial \Delta F / \partial T = -87.9$ cal./°K. determined by Tomlinson and reported by Spice et al. These numbers appeared to be the best available and were used by Goldberger and Othmer (*19*) in a recent paper on the kinetics of nickel carbonyl formation. At the lower temperatures of interest, there is a tendency for the kinetics of nickel deposition to be partially affected by thermodynamic limitations, and careful attention to this possibility should be exercised in experimental studies or plant operation.

EXPERIMENTAL TECHNIQUES

The experimental procedure and equipment are essentially those used in the studies with iron carbonyl (*1*). Each deposition experiment was conducted on a resistance-heated ⅛-in. O.D. tubular deposition element supported horizontally in a ½-in. wide rectangular orifice. Nickel carbonyl vapor, sometimes diluted with carbon monoxide, argon, or helium, was

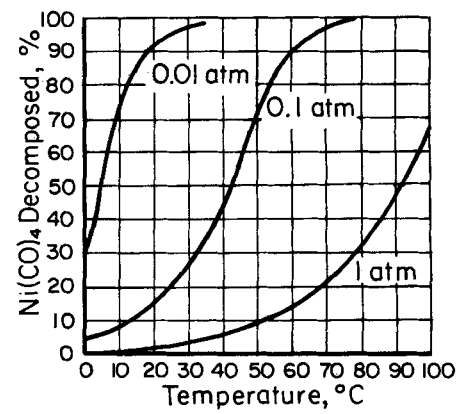

Fig. 1. Equilibrium decomposition of nickel tetracarbonyl.

passed at a measured rate and pressure through the orifice and over the deposition surface. The flow was horizontal and directed perpendicular to the axis of the heated elements. Temperatures were measured by means of a thermocouple located within the tubular element in the center of the deposition assembly. Since the temperature drop across the wall of the elements was less than 1°, no correction was necessary for the thermocouple position. The deposition rate was determined by weight gain, the initial surface area, and the length of the run.

The nickel carbonyl in high-pressure cylinders was obtained from the International Nickel Company. The hydrogen was diffused through palladium. The other gases were of commercially available high purity grade sold in compressed gas cylinders and were used without further purification. The deposition elements were low carbon steel or nickel tubing of commercial grade. A new filament, cleaned with abrasive cloth, was used in each experiment. Immediately before a deposition experiment, the filament was heated to 530°C. in flowing hydrogen in the deposition apparatus. This procedure was found necessary in previous studies to nucleate carbonyl iron on steel filaments and was continued in the carbonyl nickel experiments. The use of either steel or nickel as the filament material gave essentially the same rate of deposition of carbonyl nickel, but the adherence of the nickel deposits to nickel substrates was significantly higher than the adherence of nickel deposits to steel substrates.

EXPERIMENTAL RESULTS

Samples of the deposition rate data are presented in Table 1. The first three experiments illustrate the effect of temperature on the rate in the kinetically controlled region, the fourth example illustrates the effect of natural convection, and the last four experiments show the effect of diluents in the diffusion-controlled region. Additional data are presented in the figures, which show in more detail the effects of the various variables.

No gas phase, or homogeneous, nucleation was observed in any of the present experiments. The maximum temperature of 225°C. used in these nickel carbonyl experiments was purposely kept below the 248° to 305°C. temperature range previously found to result in homogeneous nucleation in the iron carbonyl system. All the nickel carbonyl data should therefore be free of homogeneous nucleation constraints.

The effect of temperature on the deposition rate for undiluted feed is graphically illustrated in Figure 2. The rate is exponentially dependent at low temperatures but becomes relatively insensitive to temperature above about 175°C., despite the fact that the conversion levels in all cases are below 8%. Since thermodynamics is certainly not limiting, and since there is still ample reactant available for reaction, it appears that a temperature level of about 175°C. separates the diffusion-controlled region from the kinetically controlled region under the experimental conditions employed in this study.

TABLE 1. DEPOSITION RATE DATA

Experiment No.	Rate, g./(sq. cm.)(hr.)	Total pressure, torr	Reynolds number	Grashof number	Filament temp., °C.	Added diluent Species	Vol. %
148	0.083	20	17	17	125	—	0
152	0.24	20	16	14	150	—	0
150	0.58	20	14	11	175	—	0
192	0.81	200	14	1,050	175	—	0
188	2.2	50	64	50	225	—	0
182	0.82	50	13	6	225	Argon	72
187	0.68	50	10	1	225	Helium	84
184	0.51	50	18	4	225	Carbon monoxide	83

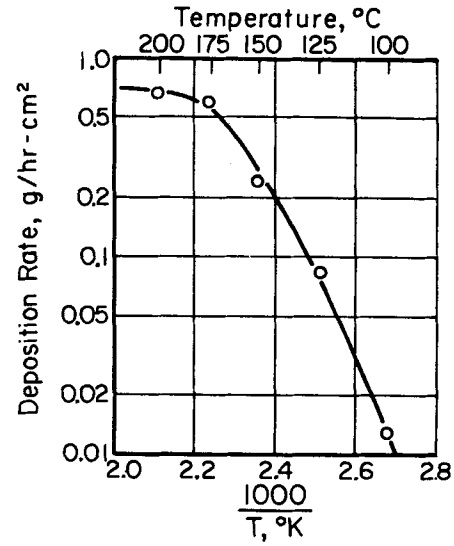

Fig. 2. Effect of temperature on decomposition rate of nickel at a Reynolds number of about 15 and a pressure of 20 torrs.

These two regions of control can be further identified by the effect of diluents on rates at a constant mass flow of carbonyl, as shown in Figure 3. At low temperatures the deposition rate with carbon monoxide diluent is reduced significantly more than the reduction obtained with an equivalent amount of argon, suggesting a strong retarding effect on the surface reaction by adsorbed carbon monoxide. This is not believed to be a thermodynamic effect, since the addition of argon should increase yields if equilibrium were being approached.

At high temperatures, the addition of carbon monoxide gives nearly the same result as an equivalent argon dilution. Helium additions least affect the deposition rate. Helium, of course, has a significantly higher diffusivity than does argon, while argon and carbon monoxide have very similar diffusivities. At the same time, all diluents would be expected to decrease the effective concentration gradient of carbonyl to a degree roughly proportional to the amount of diluent present. The order of rate retardation and the closeness of the curves therefore suggest diffusion control with a small residual kinetic contribution at a temperature of 225°C.

In the kinetically controlled region, one would expect only a small effect of flow on reaction rate, while in the

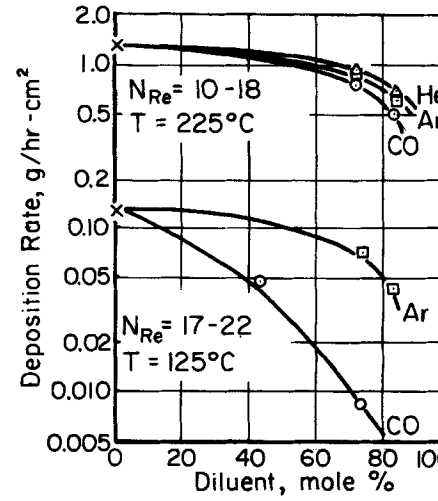

Fig. 3. Effect of diluent on deposition rate of nickel at 50 torrs total pressure.

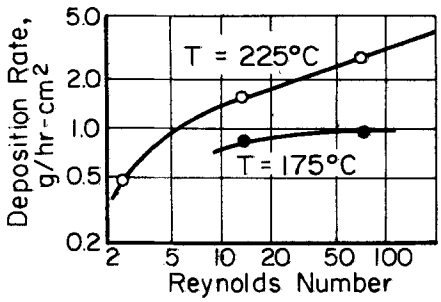

Fig. 4. Effect of flow rate on nickel deposition rate at 50 torrs total pressure.

diffusion-controlled region the deposition rate should be dominated by flow conditions. These expected interrelationships are supported by the data shown in Figure 4. At 175°C. there is only a small correlation between flow rate and reaction rate, while at 225°C. the reaction rate becomes quite sensitive to flow rate.

An attempt to show the effect of pressure on the raw deposition rate data is presented in Figure 5. This approach is not particularly rewarding because of the compounding effects introduced by partial mass transfer control, even in the so-called kinetically controlled region. This is especially difficult when natural convection is an important determinant of the flow field. Under these conditions, the interfacial partial pressures are controlled not only by the rate at which a component diffuses in a given partial pressure gradient, but also by the magnitude of the transport coefficient, which is a function of total pressure. As the pressure is increased, the convective currents as well as the bulk stream partial pressures increase, which masks the effect of pressure, per se, on surface kinetics. A considerable effort was therefore made to separate these effects in order to determine the true reaction order based on interfacial partial pressures.

CORRELATION OF RESULTS

Brown and Marco (*20*) pointed out that the square root of the Grashof number is effectively a Reynolds number for natural convective flow systems. This concept was extended by Gilmour (*21*) to the j factor relationships originally derived by Chilton and Colburn (*22*) for forced convection. By following these leads, the data based on the separate correlations of McAdams (*23*) for forced convection at $N_{Re} < 10^3$ (corrected for Prandtl number)

$$N_{Nu}/N_{Pr}^{1/3} = 0.35 + 0.49\,N_{Re}^{0.52} \qquad (2)$$

and natural convection at $N_{Gr}N_{Pr} > 10^3$

$$N_{Nu} = 0.53\,N_{Gr}^{0.25}\,N_{Pr}^{0.25} \qquad (3)$$

at a cylindrical surface were replotted as log $N_{Nu}/N_{Pr}^{1/3}$

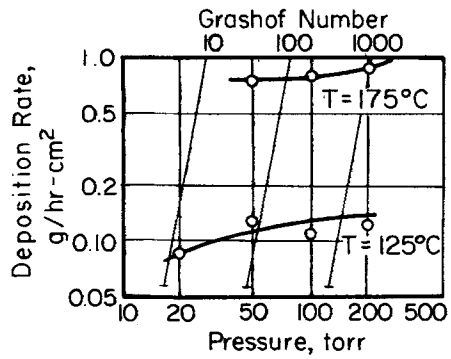

Fig. 5. Effect of pressure on deposition rate of nickel at a Reynolds number of about 20.

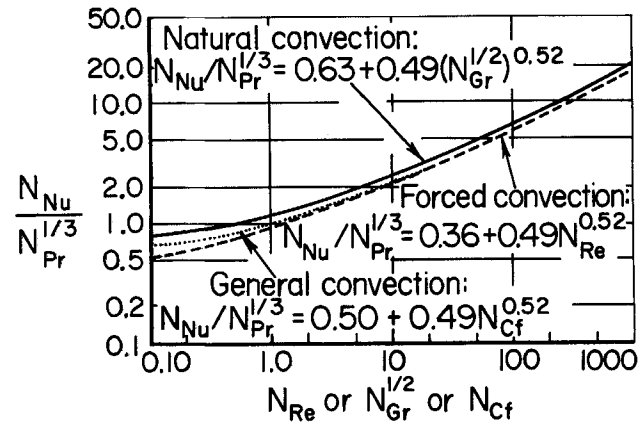

Fig. 6. Heat transfer correlations of natural- and/or forced-convection flow over a cylindrical surface.

vs. log N_{Re} or $N_{Gr}^{1/2}$, as shown in Figure 6. It can be seen that the natural convection curve, represented adequately by the expression

$$N_{Nu}/N_{Pr}^{1/3} = 0.63 + 0.49\,(N_{Gr}^{1/2})^{0.52} \qquad (4)$$

is almost within the experimental error of the data. An appropriate correlation for both types of flow is therefore

$$N_{Nu}/N_{Pr}^{1/3} = 0.50 + 0.49\,N_{Cf}^{0.52} \qquad (5)$$

since substitution of either N_{Re} or $N_{Gr}^{1/2}$ for N_{Cf} yields the correct value of N_{Nu}. A simple arithmetic average has been used for the first term of Equation (5), since the accuracy of the limited low N_{Re} or N_{Gr} data does not permit other possible methods of averaging to be evaluated; in addition it provides an adequate degree of accuracy over the range of conditions studied.

The method of combining the flow and transport parameters of a combined forced and natural convective system was based on an extension of a proposal of Tsubouchi and Sato (*24*) to combine the Reynolds and Grashof numbers vectorially. The general case can be represented by the expression

$$N_{Cf} = \sqrt{(N_{Re}\sin\theta)^2 + (N_{Re}\cos\theta + N_{Gr}^{1/2})^2} \qquad (6)$$

where θ is the angle between the vectors of the forced and natural convection flow fields. For horizontal flow used in the present study, $\theta = 90°$ and Equation (6) reduces to

$$N_{Cf} = \sqrt{N_{Re}^2 + N_{Gr}} \qquad (7)$$

With this as the combined flow parameter, the previously

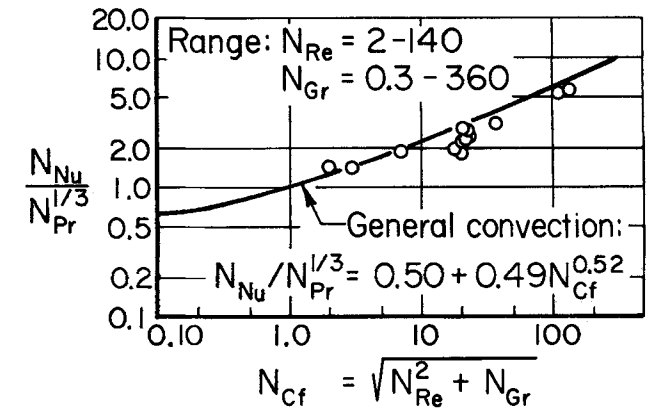

Fig. 7. Heat transfer data obtained in experimental reactor system with hydrogen and argon gases used.

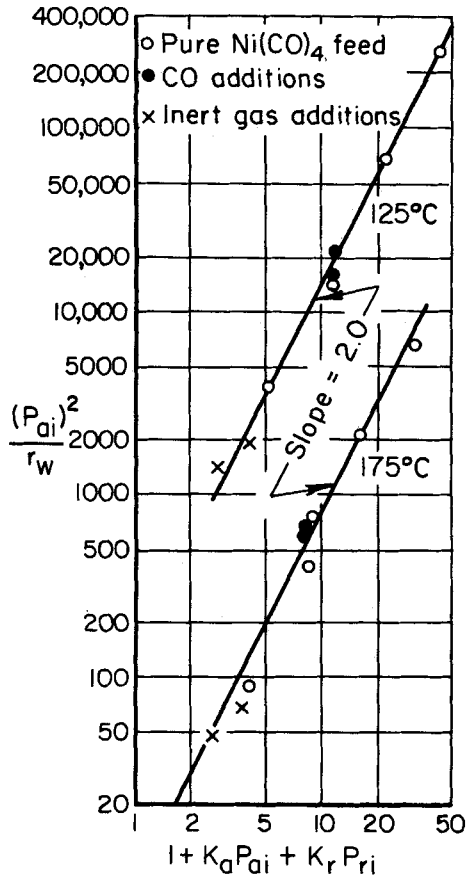

Fig. 8. Correlating curves for second-order reaction.

presented heat transfer data (*1*) are replotted in Figure 7. A decided improvement at low flow rates was obtained, although at higher flows the data were a little below the vectorially combined modified McAdams curve. Although the McAdams Nusselt-Reynolds number correlation was originally derived from data obtained with air, by including the Prandtl number raised to the one-third power, the modified curve should also be valid for nickel carbonyl and its mixtures within the accuracy of either set of data. The Prandtl number of nickel carbonyl was estimated to be about 0.93 ($N_{Pr}^{1/3} = 0.98$) from the Eucken equation (*25*) and its known heat capacity (*18*), as compared with the value of 0.69 ($N_{Pr}^{1/3} = 0.89$) for air.

This combined heat transfer correlation was converted to a mass transfer basis by use of the Chilton-Colburn analogy, and the drop in partial pressure of reactants and products over an effective film resistance around the cylindrical element was calculated from the expressions

$$r_w = M_w k_g \Delta y \tag{8}$$

with

$$k_g = [D_{ar} P N_{Sc}^{1/3} M_f / dRTM_b] \\ [0.50 + 0.49 [N_{Re}^2 + N_{Gr}]^{0.26}] \tag{9}$$

For four-to-one counterdiffusion of two components in binary systems (*26*)

$$\Delta y = 1/3 \ln \left[\frac{1 + 3y_{ab}}{1 + 3y_{ai}} \right] \tag{10}$$

and Gilliland's solution for a ternary system (*27*)

$$\Delta y = 1/3 \ln \left[\frac{(1/D_{ar} - 1/D_{rc})\, y_{ab} + (1/D_{ar} - 1/D_{ac})\, y_{rb}/4 + (1/D_{ac} - 1/D_{rc})/3}{(1/D_{ar} - 1/D_{rc})\, y_{ai} + (1/D_{ar} - 1/D_{ac})\, y_{ri}/4 + (1/D_{ac} - 1/D_{rc})/3} \right] \tag{11}$$

By the use of these expressions and calculated diffusivities based on estimated Leonard-Jones force constants by the method of Hirschfelder et al. (*28*), the interfacial partial pressures of the reactants were calculated from the bulk stream values. These interfacial values were then used to test various models for rate limiting surface kinetics, including adsorption of carbonyl, tetracarbonyl decomposition, lower carbonyl decomposition, and desorption of carbon monoxide following the procedures of Hougen and Watson (*29*) for applying the Langmuir-Hinshelwood (*30, 31*) adsorption surface reaction rate isotherms. The best model was based on a second-order surface reaction of adsorbed tetracarbonyl involving two adjacent sites. The ability of this model to correlate experimental data is shown graphically in Figure 8. The regression analysis of the experimental data is actually based on linearized forms of the kinetic expression, which does not necessarily give the best values for the reaction rates. By additional hand manipulation of the constants, slightly better expressions can be obtained. The final recommended equation and the standard deviation at 125°C. are

$$r_w = \frac{0.0072(P_{ai})^2}{(1 + 0.21 P_{ai} + 0.22 P_{ri})^2}, \sigma = 16\% \tag{12}$$

and at 175°C.

$$r_w = \frac{0.13 (P_{ai})^2}{(1 + 0.19 P_{ai} + 0.13 P_{ri})^2}, \sigma = 21\% \tag{13}$$

It should be noticed that at higher pressures (~100 torrs), an apparent zero-order behavior is expected, while at low pressures (~1 torr), the second-order dependence becomes apparent. At intermediate pressures, approximately first-order behavior would be exhibited. The adsorption coefficients for argon and helium were found to be negligible under all experimental conditions.

On the assumption that the coefficients in the equations are exponential functions of reciprocal temperature, these two equations can then be combined into a general equation valid over an extended temperature range:

$$r_w = \frac{k_o k_a^2 \exp - E_o/RT \exp 2E_a/RT [P^2_{ai} - (P^4_{ri}/K_{eq})^2]}{[1 + k_a \exp E_a/RT\, P_{ai} + k_r \exp E_r/RT\, P_{ri}]^2} \tag{14}$$

where

$k_o = 1.8 \times 10^{11}$ g./(hr.)(sq. cm.)
$k_a = 8.9 \times 10^{-2}$ torr^{-1}
$k_r = 1.52 \times 10^{-3}$ torr^{-1}
$E_o = 21{,}900$ cal./g.-mole
$E_a = 700$ cal./g.-mole
$E_r = 4{,}000$ cal./g.-mole

Three additional data points, which were not used in establishing Equation (14), are available to check the accuracy of this rate expression. For single data points at 100° and 150°C., Equation (14) agrees with 5% of the experimental rates. At 200°C., where the rate is heavily controlled by diffusion, the agreement is only 75%, but this deviation is not unexpected, since the error in subtracting the diffusion resistance has been greatly magnified in the kinetic analysis. Simultaneous solution of the kinetic and diffusional equations for temperatures in the 200°C. range yields a satisfactory rate prediction.

The effect of diluents on the nickel carbonyl reaction at low temperatures, and hence in the kinetically controlled region, is therefore quite different from their effect on the

iron carbonyl reaction studied previously. In the iron carbonyl study, diluents added to a constant carbonyl flow increased the rate of reaction, while in the present study the rates were reduced. For a first-order reaction with a dual-site mechanism

$$r = K_o'P_a/(1 + K_aP_a + K_rP_r)^2 \qquad (15)$$

r increases as P_a and P_r approach zero (by dilution) when K_aP_a and K_rP_r are much greater than unity. This was the model found to best represent the iron carbonyl system.

However, in the nickel carbonyl system, a reaction order equal to or greater than the number of sites involved is necessary to explain the decrease in rate with partial pressure, that is

$$r = K_o'P_a^m/(1 + K_aP_a + K_rP_r)^n \qquad (16)$$

where r approaches zero as P_a and P_r approach zero (by dilution) when $m \geq n$ for all values of K_aP_a and K_rP_r.

The major contrast of this study and previous work is in the order of the reaction. Bawn (6), Garratt and Thompson (7), and Tonosaki (8) reported first-order behavior at low temperatures and at pressure levels corresponding to the intermediate pressure range discussed previously, where apparent first-order effects would be expected. Chan and McIntosh (9) correlated their heterogeneous results with an equation which corresponds to a first-order single-site reaction model. However, their maximum temperatures were only about 80°C. It should be obvious that temperature as well as pressure can change the apparent and perhaps true order of a reaction, and first-order behavior becomes an increasingly better approximation as temperature is decreased.

The heterogeneous rates measured by Chan and McIntosh are much less than the rates indicated by Equation (14). This difference may be due to lower effective surface areas of their low-temperature bright deposits as compared with the high surface area dull deposits obtained in the present studies. In addition, heating of the glass wool in the bulb employed by Chan and McIntosh was by transfer through the low-pressure deposition gases. Since the reaction requires 35,000 cal./g.-mole, their deposition-surface temperatures were probably significantly below the measured temperatures.

Tewes, Zava, and Hoover (10) reported two data points which can be used to test Equation (14), and it was found that their data could be predicted within a few percent, that is well within the experimental error. Boettger and Fetting (11) used a feed of 1% nickel carbonyl in nitrogen, and because of this high dilution and somewhat less favorable transport geometry, they encountered appreciable diffusion resistances at temperatures as low as 100°C. Assuming a first-order reaction, they obtained an apparent activation energy of 17,000 cal./g.-mole, which agrees fairly well with the apparent value of about 20,000 cal./g.-mole obtained in the present studies.

CONCLUSIONS

1. The deposition rate of nickel from its carbonyl is affected by both diffusion and kinetics in the range of conditions of practical interest. In the system employed in this study, a temperature level of about 175°C. separated the two regions of control.

2. The rate limiting step in the chemical reaction appears to be best represented by a second-order two-site decomposition of absorbed nickel tetracarbonyl with an activation energy of about 22,000 cal./g.-mole.

3. The carbonyl is apparently only physically adsorbed with an apparent heat of adsorption of about 700 cal./g.-mole.

4. Carbon monoxide is more strongly bonded to the surface with an apparent heat of adsorption of about 4,000 cal./g.-mole.

5. Argon and helium are not significantly adsorbed on carbonyl nickel during deposition, and their presence does not affect the chemical kinetics except as they change the partial pressure of the reactants at the reaction interface.

ACKNOWLEDGMENT

The authors express their appreciation to the companies who cooperatively sponsored the fundamental program on chemical vapor deposition at Battelle Memorial Institute for their financial support. We thank Dr. J. M. Blocher, Jr., and A. C. Loonam, who encouraged and contributed to this work, and Mrs. Joann Bossenbroek, who assisted in computer programming.

NOTATION

c_p = specific heat at constant pressure, cal./(g.)(°K.)
d = filament diameter, cm.
D_{jk} = diffusivity of mixture of j^{th} and k^{th} components, sq. cm./hr.
E_j = adsorption energy, cal./g.-mole
E_o = activation energy, cal./g.-mole
G = mass flow rate, g./(hr.)(sq. cm.)
g = gravitational constant, 1.27×10^{10} cm./hr.^{2}
h = heat transfer coefficient, cal./(hr.)(sq. cm.)(°K.)
K_j = adsorption constant, torr^{-1}
K_{eq} = equilibrium constant for nickel carbonyl decomposition, exp (64.2 — 10,500/T) torr^3
K_o = rate constant, g./(hr.)(sq. cm.)
k_j = adsorption coefficient, torr^{-1}
k = thermal conductivity of gas, cal./(cm.)(hr.)(°K.)
k_g = mass transfer coefficient, g.-moles/(sq. cm.)(hr.)
k_o = rate coefficient, g./(sq. cm.)(hr.)
M = molecular or atomic weight, g./g.-mole
N_{Cf} = combined flow parameter, $\sqrt{N_{Re}^2 + N_{Gr}}$
N_{Gr} = Grashof number, $d^3g\,(\rho_f/\mu_f)^2\,(\rho_b - \rho_i)/\rho_b$
N_{Nu} = Nusselt number, hd/k_f
N_{Pr} = Prandtl number, $c_p\mu_f/k_f$
N_{Re} = Reynolds number, dG/μ_f
N_{Sc} = Schmidt number, $\mu_f/D_f\rho_f$
N_{Sh} = Sherwood number, k_gdRT/D_fP
m = order of reaction
n = number of sites involved in surface reaction
P = total pressure, torr
P_{ji} = partial pressure at interface, torr
R = gas constant, cal./(g.-mole)(°K.) or (cc.)(torr)/(g.-mole)(°K.)
r_w = deposition rate, g./(hr.)(sq. cm.)
T = temperature of deposition system, °K.
y_{jb} = mole fraction in bulk stream
y_{ji} = mole fraction at interface
Δy = diffusion potential, defined by Equations (10) and (11)
θ = angle between forced and natural convective flow vectors, deg.
μ = gas viscosity, g./(cm.)(hr.)
ρ = gas density, g./cc.
σ = standard deviation

Subscripts

a = value for carbonyl
b = bulk stream value
c = value for argon diluent
d = value for helium diluent
f = film value
i = interfacial value
j = value for j^{th} component
k = value for k^{th} component
r = value for carbon monoxide
w = value for nickel

LITERATURE CITED

1. Carlton, H. E., and J. H. Oxley, *A.I.Ch.E. J.*, **11**, 79 (1965).
2. "Threshhold Limit Values for 1964," Am. Conf. Government-Industrial Hygenists.
3. Mond, L., U. S. Pats. 455,227-455,230 (June 30, 1891).
4. *Ind. Chem.*, **35**, 583 (1959).
5. Mittasch, A., *Z. Phys. Chem.*, **40**, 1 (1902).
6. Bawn, C. E. H., *Trans. Faraday Soc.*, **31**, 440 (1935).
7. Garratt, A. P., and H. W. Thompson, *J. Chem. Soc. London*, 1822 (1934).
8. Tonosaki, Koichi, *Sci. Rept.* Tohoku Univ., First Serv., **37**, 39 (1953).
9. Chan, R. K., and R. McIntosh, *Can. J. Chem.*, **40**, 845 (1962).
10. Tewes, W. E., T. E. Zava, and T. B. Hoover, *USAEC Rept. K-1533* (Nov. 23, 1962).
11. Boettger, G., and F. Fetting, *Chem. Ingr. Tech.*, **34**, 384 (1962).
12. Verblovskii, A. M., and A. L. Rotinian, *Zh. Prikl. Khim.*, **33**, (1), 102 (1960).
13. Owen, L. W., *Metallurgia*, **59**, 165, 227, 295 (1959).
14. Callear, A. B., *Proc. Roy. Soc.*, **265**, 71 (1961).
15. Mond, R., *J. Soc. Chem. Ind.*, **49T**, 371 (1930).
16. Belozerskiy, N. A., "Karbonily Metallov," Moscow (1958).
17. Powell, C. F., I. E. Campbell, and B. W. Gonser, "Vapor Plating," Wiley, New York (1955).
18. Spice, J. E., L. A. K. Staveley, and G. A. Harrow, *J. Chem. Soc.*, 100 (1955).
19. Goldberger, W. M., and D. F. Othmer, *Ind. Eng. Chem. Process Design Develop.*, **2**, 203 (1963).
20. Brown, A. I., and S. M. Marco, "Introduction to Heat Transfer," 2 ed., McGraw-Hill, New York (1951).
21. Gilmour, C. H., in "Chemical Engineers' Handbook," R. W. Perry, C. H. Chilton, and S. D. Kirkpatrick, ed., Sect. 10, McGraw-Hill, New York (1963).
22. Chilton, T. H., and A. P. Colburn, *Ind. Eng. Chem.*, **26**, 1183 (1934).
23. McAdams, W. H., "Heat Transmission," 3 ed., McGraw-Hill, New York (1954).
24. Tsubouchi, T., and S. Sato, *Chem. Eng. Progr. Symposium Ser. No. 30*, **56**, 285 (1960).
25. Reid, R. C., and T. K. Sherwood, "The Properties of Gases and Liquids," McGraw-Hill, New York (1948).
26. Colburn, A. P., and T. B. Drew, *Trans. Am. Inst. Chem. Engrs.*, **33**, 197 (1937).
27. Sherwood, T. K., "Absorption and Extraction," 1 ed., McGraw-Hill, New York (1937).
28. Hirschfelder, J. O., C. F. Curtis and R. B. Bird, "Molecular Theory of Gases and Liquids," Wiley, New York (1954).
29. Hougen, O. A., and K. M. Watson, "Chemical Process Principles," Pt. 3, Wiley, New York (1947).
30. Langmuir, I., *Trans. Faraday Soc.*, **17**, 621 (1921).
31. Hinshelwood, C. N., "Kinetics of Chemical Changes," Oxford Univ. Press, New York (1926).

Manuscript received July 19, 1965; revision received May 23, 1966; paper accepted May 25, 1966.

Gas Absorption by Drops Traveling on a Vertical Wire

SHANTI MOHAN RAJAN and SIMON L. GOREN

University of California, Berkeley, California

In the measurement of the absorption of carbon dioxide gas by a series of oil drops moving down a vertical wire the variables studied are drop frequency, oil viscosity, wire size, and column length. A model is proposed which assumes that the gas is absorbed by almost stagnant liquid film between and covering the drops, that the film is subsequently mixed with a drop as it moves past, and that the dissolved gas is carried from the column in circulating loops of liquid within the drops. The model leads to an equation which correlates the data and gives a good approximation to the slope of the line.

This study is concerned with the liquid-side controlled absorption of carbon dioxide gas by a series of white oil drops moving down a vertical wire. Adjacent drops are connected to each other by a thin liquid film, and both the drops and film are axisymmetric about the wire. Inside each drop is a circulating loop of liquid roughly in the shape of a torus. Throughout this paper, *drop* is used to denote the combination of the circulating torus with the region surrounding it to form the observed bulge; *torus* refers to the circulating loop only.

Figure 1 gives the geometry of the flow and also defines the nomenclature used. Figure 2c is a schematic rep-